Optical Recharge of Anisotropic Impurity Centers in Garnets in Spatially Inhomogeneous Light Fields.

I. I. Davidenko
Kiev Taras Shevchenko National University, Ukraine
daviden@ukrpack.net

M. Fally and R. A. Rupp
Institute of Experimental Physics, Vienna University, Austria
Martin.Fally@exp.univie.ac.at, Romano.Rupp@exp.univie.ac.at

Abstract: The reason for the appearance of magnetic and optical anisotropy in garnets under the influence of spatially inhomogeneous light fields is investigated. The superposition of two coherent linearly polarized beams with either mutually orthogonal or parallel polarization vectors is considered. The resulting magnetic and optical anisotropy is related to an optical recharge of anisotropic impurity centers localized in crystal sites with different environment symmetry. The electron excitation and transitions under the influence of illumination are studied for the magnetic YIG:Co garnet and the paramagnetic CaMnGe garnet. A theoretical model of the occupancies' kinetics of such centers is developed. The dynamics and spatial distribution of the energy of the photoinduced magnetic anisotropy for the YIG:Co as well as time and angular dependence of photoinduced birefringence in CaMnGe garnet are calculated. The results are compared with the corresponding experiments.
OCIS codes: (260.1440) Birefringence, (160.0160) Materials.

Introduction

A wide class of the photoinduced effects (PIE) existing in different magnetic and non-magnetic materials is known and widely investigated now. PIE dependent on the polarization state of the incident light, such as magnetization reversals (photoinduced spin-reorientation transitions) [1-3] and changes of optical anisotropy (photoinduced linear birefringence) [4,5] are considered as perspective for the practical applications. These effects happen under influence of linearly polarized light and their features are determined by the illumination conditions. Garnets of different compositions were employed usually as the model objects for study of PIE due to their well investigated electrical, optical and magnetic properties. This circumstance allows to interpret adequately and to explain the results of experimental observations of PIE at the phenomenological and microscopic levels. The main problem of practical applications of PIE till now was connected with low (cryogenic) temperatures of their existence. The recent discovery of PIE at room temperature in yttrium-iron garnet doped with cobalt (YIG:Co) [2,3] and the relative simplicity of forming magnetic or optical anisotropy under illumination with linearly polarized light open a perspective for the practical use of PIE, e.g. for information storage and processing or for optoelectronic devices.

The aim of the present work is to develop a theoretical basis and to demonstrate possibilities to form magnetic and non-magnetic holographic gratings in garnets of different compositions exposed by spatially inhomogeneous light fields being a superposition of two coherent linearly polarized beams with mutually orthogonal or parallel polarization vectors. YIG:Co is considered as an example of medium with photomagnetic properties and manganese-germanium garnets (MGG) is used for investigations of the photoinduced linear birefringence (PLB). A possibility of formation of the magnetic holographic grating in YIG:Co is predicted. Perspectives of further utilization of the developed theoretical model is discussed.

Model

According to the modern concepts [1-3,6] the physical nature of PIE in garnets is connected with the presence of highly anisotropic ions in octahedral sites of the garnet crystal lattice: Fe^{2+} in yttrium-iron garnet doped with silicon (YIG:Si), Co^{2+} in YIG:Co and Mn^{3+} in MGG. These ions create essential trigonal distortions of ligand environment in the octahedral sites due to their orbital degeneracy, thus reducing the site symmetry. The symmetry of the garnet still remains 4/m with four differently oriented sites of the trigonal Wykoff symmetry. The trigonal axis $<111>_i$ (i=1,2,3,4) is one of the principal axes of the electric dipole moment.

At the absence of external treatments all four types of the octahedral sites are equally occupied with the highly anisotropic ions. Under an influence of linearly polarized light an excitation of those ions occurs. Furthermore, the probability for a photoexcitation of the ion depends on the angle between the dipole moment of electron transition and the light polarization vector. On the other hand, the direction of dipole moment of electron transition is hardly connected with the electric dipole moment in the initial state, i.e. with the orientation of the local trigonal axis $<111>_i$. Thus, the probability of a photoexcitation of the active centers is different for different octahedral sites [5]. After excitation the electron transition from octahedral site where the light quantum was absorbed to another one is possible. In the excited site ions in another valence state remain: $Fe^{2+}\rightarrow Fe^{3+}$ (YIG:Si), $Co^{2+}\rightarrow Co^{3+}$ (YIG:Co), $Mn^{3+}\rightarrow Mn^{4+}$ (MGG). These Fe^{3+}, Co^{3+} and Mn^{4+} ions are characterized by essentially lower anisotropy per one ion as compared to Fe^{2+}, Co^{2+} and Mn^{3+}. Thus, effective redistribution of the occupancies of the octahedral sites with anisotropic ions occurs. Such redistribution shows itself in the appearance of a photoinduced optical or/and magnetic anisotropy. In magnetic garnets formation of the photoinduced magnetic anisotropy (PMA) is considered as a reason of experimentally observed magnetization reversals.

The same approach can be used for studying of PIE in garnets exposed to a superposition of two coherent linearly polarized light beams $\vec{e}_1 = \vec{A}_1 \exp[-i\varepsilon_1]$ and $\vec{e}_2 = \vec{A}_2 \exp[-i\varepsilon_2]$ as it takes place when recording holographic gratings (see Fig.1). Two limiting situations can be realized: orthogonal or parallel orientations of the polarization vectors resulting respectively in a spatial modulation of the polarization or intensity of the light along the sample surface restectively. In both cases we consider the electron transition between the states S_1 and S_2 without concrete definition of their physical nature. However, it is straightforward to suppose, that S_1 is the ground state of the ions in an octahedral site with the direction of the dipole moment along the local trigonal axes $<111>_i$.

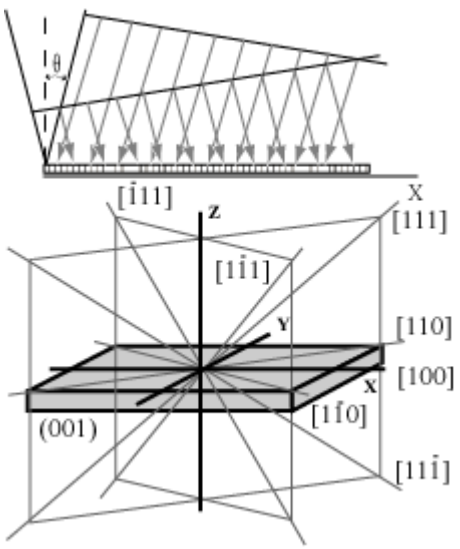

Fig.1. Illumination of the garnet sample with two coherent linearly polarized light beams.

When the sample is illuminated with two coherent light beams with $\vec{e}_1 \perp \vec{e}_2$ the polarization of the total incident light wave changes along the sample surface from elliptical through circular to elliptical with another orientation of the polarization ellipse [7]. Geometric configuration of the sample in the (001) plane is similar to the experimental ones for YIG:Co [2,3] and MGG [5,7]. Mutual orientation of two linearly polarized components of the elliptically polarized total light wave with amplitudes $\vec{A}_1$ and $\vec{A}_2$, trigonal axis $<111>_i$ and components of the radius-vector of the electron transition are shown schematically in Fig.2.

Neglecting the finite lifetime in the excited state the probability of photoabsorption per unit of time υ_i of the ion in the dipole approximation can be expressed by:

$$\upsilon_i = \frac{2\pi^2}{\hbar c}\Big[\left\langle S_2 \left| \vec{e}_{1\|} \cdot \vec{d}_i \right| S_1 \right\rangle^2 \delta(f_{12}-f) + \left\langle S_2 \left| \vec{e}_{1\perp} \cdot \vec{d}_i \right| S_1 \right\rangle^2 \delta(f_{12}-f) + \left\langle S_2 \left| \vec{e}_{2\|} \cdot \vec{d}_i \right| S_1 \right\rangle^2 \delta(f_{12}-f) + \left\langle S_2 \left| \vec{e}_{2\perp} \cdot \vec{d}_i \right| S_1 \right\rangle^2 \delta(f_{12}-f) \Big] \quad (1)$$

where $\vec{e}_{1\|}, \vec{e}_{1\perp}, \vec{e}_{2\|}$ and $\vec{e}_{2\perp}$ are the components of the light beams $\vec{e}_1$ and $\vec{e}_2$ along and perpendicular to the $<111>_i$ direction, $\vec{d}=-e\vec{r}$ is the dipole moment of the electron transition, $\left\langle S_2 \left| \vec{e}_{1\|} \cdot \vec{d}_i \right| S_1 \right\rangle^2$, $\left\langle S_2 \left| \vec{e}_{1\perp} \cdot \vec{d}_i \right| S_1 \right\rangle^2$, $\left\langle S_2 \left| \vec{e}_{2\|} \cdot \vec{d}_i \right| S_1 \right\rangle^2$ and $\left\langle S_2 \left| \vec{e}_{2\perp} \cdot \vec{d}_i \right| S_1 \right\rangle^2$ are the matrix elements of the dipole moment of the electron transition from the state S_1 into the state S_2 with the corresponding frequency f_{12}. Taking into account the notation introduced in Fig.2 we rewrite Eq.(1) to:

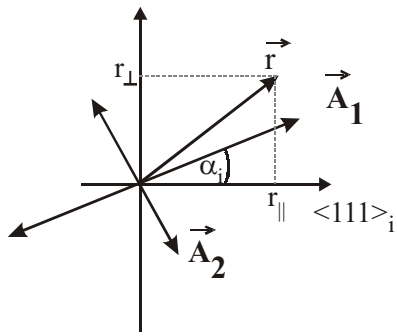

Fig.2. Influence of the elliptically polarized light on the photoactive octahedral site.

$$\upsilon_i = \frac{2\pi^2}{\hbar c} e^2 \left[|\vec{e}_1|^2 \cos^2\alpha_i r_{i\perp}{}^2 + |\vec{e}_1|^2 \sin^2\alpha_i r_{i\|}{}^2 + |\vec{e}_2|^2 \sin^2\alpha_i r_{i\perp}{}^2 + |\vec{e}_2|^2 \cos^2\alpha_i r_{i\|}{}^2 \right] \quad (2)$$

where $r_{i\perp} = \left\langle S_2 \left| r_\perp \right| S_1 \right\rangle$ and $r_{i\|} = \left\langle S_2 \left| r_\| \right| S_1 \right\rangle$ are the matrix elements of the radius-vector. After a rearrangements following expression for υ_i is obtained:

$$\upsilon_i = AI[1+B\cos^2\alpha_i + \chi(1+B\sin^2\alpha_i) \quad (3)$$

where $A=\frac{2\pi^2}{\hbar c} e^2 r_{i\perp}{}^2$, $B=\frac{r_{i\|}{}^2 - r_{i\perp}{}^2}{r_{i\perp}{}^2}$ and $\chi=|\vec{e}_2| / |\vec{e}_1|$ is the ratio between the linearly polarized components of the total incident elliptically polarized light beam taking into account their phases. For magnetically ordered mediums an additional term [8] appears in Eq.(3):

$$\upsilon_i = AI[1+B\cos^2\alpha_i + \chi(1+B\sin^2\alpha_i)(1+C\cos^2\psi_i) \quad (4)$$

where ψ_i is the angle between $<111>_i$ and magnetization direction, C is a phenomenological constant. Expressions for the transition rates ω_i are deduced using Eq.(3) and (4) for non-magnetic and magnetic cases respectively, similar to the case of PIE excitation by the linearly polarized light [5,7]. The kinetics of the octahedral site occupancies n_i are described by the simplest system of kinetic equations [5,7]:

$$\frac{dn_i}{dt} = -\omega_i n_i + \frac{1}{3}\sum_{j=1}^{3} \omega_j n_j, \; i \neq j, \; \sum_{i=1}^{4} n_i = N \quad (5)$$

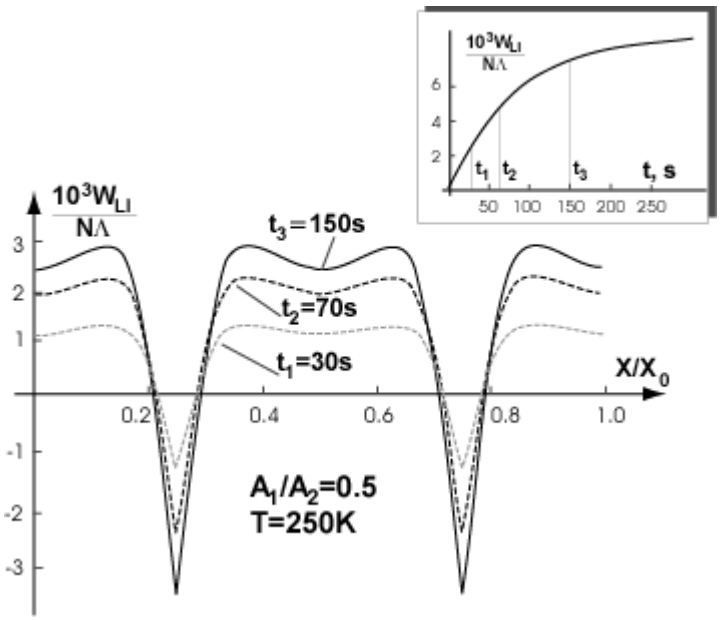

Fig.3. Numerical simulations of the spatial distribution of PMA energy in the YIG:Co film ($\vec{e}_1 \perp \vec{e}_2$) for different duration of illumination. Insert: dynamics of PMA energy in the fixed point on the sample surface.

where N is the total concentration of the photoactive octahedral centers. Further the spatial distribution of the energy of PMA induced by light wave with spatial modulation of the polarization state was calculated using the results n_i(t) of solution of the system (5) and expression for the energy of PMA [9]. Results of numerical simulations are present in Fig.3. Calculations were made for the magnetic domain with magnetization direction $\vec{M}||[111]$. The plotted results are normalized by N and a phenomenological constant Λ was used in the single ion approximation [9]. The coordinate X is normalized by the spatial period X_0.

Similar calculations earlier were made for MGG in paramagnetic state [7]. In this case Eq.(3) was used for deducing the transition rates. Due to the absence of a direction of magnetization only two types of the octahedral sites are distinguished and therefore the system (5) consists of only two equations. In contrast to the magnetic case (Fig.3) the optical anisotropy (PLB) in paramagnetic MGG is absent in the points X/X_0=0.25; 0.75 …, where the polarization state of the total beam is close to circular. The existence of magnetization involves finite values of PMA energy even in these points.

If polarization vectors of the components are parallel ($\vec{e}_1 \parallel \vec{e}_2$), then the polarization of the total light wave remains linear. Modulation of light intensity occurs at the sample surface along the X axis (see Fig.1):

$$I(X)=\left|\vec{A}_1\right|^2+\left|\vec{A}_2\right|^2+2\left|\vec{A}_1\right|\left|\vec{A}_2\right|\cos\gamma \qquad (6)$$

where $\gamma=\varepsilon_1-\varepsilon_2=\frac{4\pi}{\lambda}X\sin\theta$ (see Fig.1). As it was shown in Ref.[3], transition rates ω_i are proportional to the light intensity. Thus, spatial distribution of the photoinduced anisotropy follows the corresponding distribution of the light intensity. Results of numerical simulations of the value $(n_1-n_2)/N$ for the paramagnetic MGG in the case $\vec{e}_1 \parallel \vec{e}_2$ for different duration of illumination are shown in Fig.4. PLB is proportional to this value.

Similarly to the previous case ($\vec{e}_1 \perp \vec{e}_2$), spatial

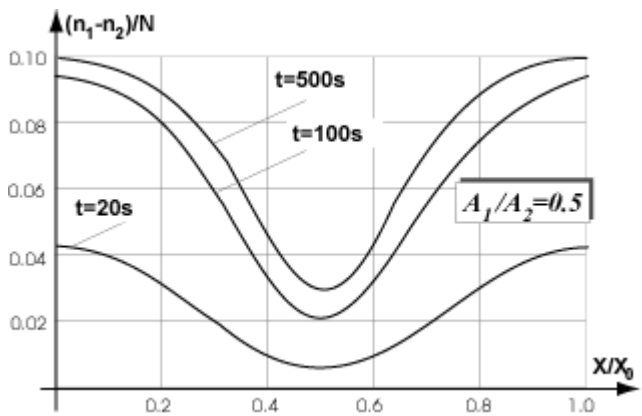

Fig.4. Numerical simulations of spatial distribution of the occupancies difference in paramagnetic MGG in the case $\vec{e}_1 \parallel \vec{e}_2$ for different duration of illumination.

heterogeneities of the rates of electron transitions for different octahedral sites cause heterogeneous spatial distribution of the photoinduced anisotropy. In both cases the depth of spatial modulation of anisotropy can be varied by changing of the ratio between the amplitudes of the linearly polarized components. The results shown in Fig.3 and Fig.4 were calculated for $A_1/A_2=0.5$.

Analysis of the experimental results

Theoretical fitting within the scope of the above developed model to the experimental results [4] obtained by measurements of the diffraction efficiency of a grating in MGG $Ca_3Mn_2Ge_3O_{12}$ was performed [7]. During recording the sample was illuminated by superposing two linearly polarized light beams with perpendicular polarization vectors, i.e. spatial modulation of the polarization state of the total light wave ocurred. A good quantitative agreement of the time [1] and angular [5] experimental dependencies was reached. This fact testify the adequacy of the developed theoretical model to the real physical processes.

A particular practical interest is connected with perspectives to holographically record a magnetic polarization holographic grating. Thin epitaxial films of YIG:Co can be considered at present as the most appropriate medium for these purposes due to the large magnitude of PIE existing within a wide temperature range, up to the room temperature [2,3]. Experimental investigations of the photoinduced spin-reorientation transitions were performed on 10 μm thickness epitaxial films $Y_2CaFe_{3.9}Co_{0.1}GeO_{12}$ grown on a paramagnetic substrate $Gd_3Ga_5O_{12}$ in the (001)-plane. Four easy magnetization-axis orientations slightly inclined from a <111> type of crystallographic direction to the sample plane exist. Magnetic-domain phases have different in-plane magnetization components. For PIE excitation the sample was illuminated with an argon laser beam (λ=488 nm, light spot radius was 50 μm) focused on the film surface in the spatial region containing a boundary between the domain phases. Magnetization reversal happens through a shift and bend of the boundary between domain phases P_A and P_C with different in-plane magnetization components (Fig.5 [2]). The effect was observed within the temperature range from liquid helium up to the room temperature.

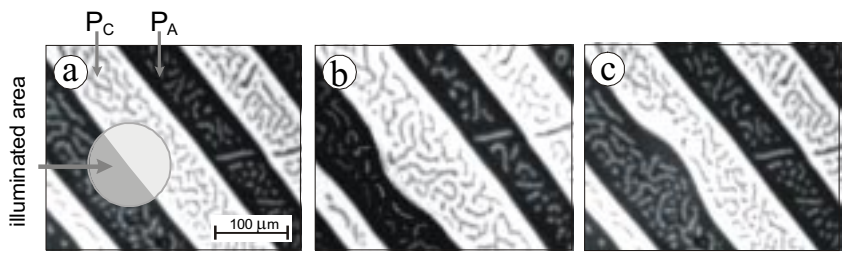

Fig.5. Pictures of the domain structure consisting of a boundary between domain phases P_A and P_C: a) before illumination; b) and c) after illumination with linearly polarized light beam with polarization vectors $\vec{E}\|[1\bar{1}0]$ and $\vec{E}\|[110]$ respectively.

The experimental technique [3] developed, experimental technique allows to estimate the value of the effective magnetic field of PMA. It essentially depends on the temperature and changes from 2 to 13 kOe while temperature is decreasing from 230K to 160K (Fig.6 [3]). These values are quite large. Simultaneously the start field of the domain wall motion was measured at the same sample [3], i.e. the strength of external magnetic field corresponding to the start of domain wall motion from the equilibrium state. This value also changes with temperature from 170 Oe to 20 Oe at the sample heating from 150K to 300K. Analyzing these results one can conclude that the magnetic field of PMA is enough for the formation

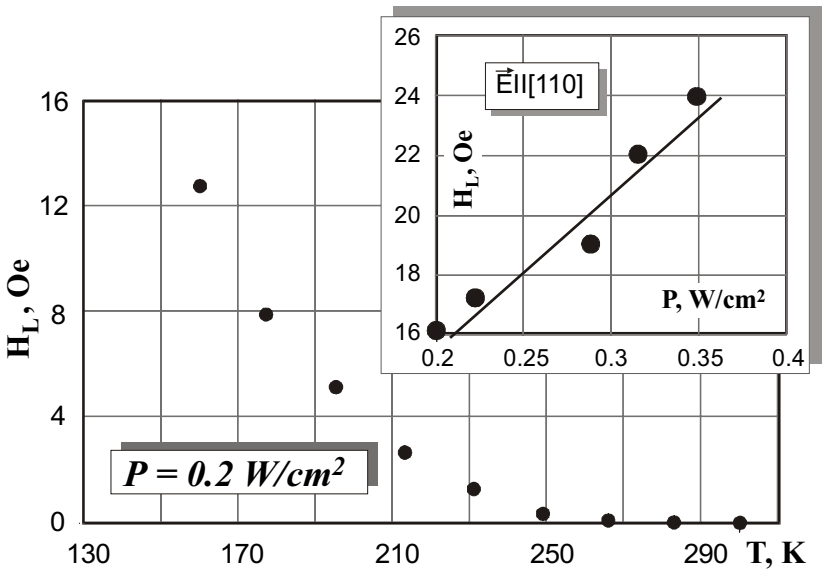

Fig.6.Experimental temperature dependency of the effective field of PMA [3]. Insert: dependency of the effective field of PMA on the light intensity at T=300K [3].

and stabilization of stripe domain structure, such as holographic grating, in the light field with spatial modulation of the polarization state or intensity. This process can be optimized by the appropriate choice of spatial period of the light field and depth of its modulation. For example, as it follows from the results of numerical simulations present in Fig.3 approximately 50% of the PMA saturation field can be reached at the ratio 0.5 between the amplitudes of the linearly polarized components in case $\vec{e}_1 \perp \vec{e}_2$ (spatial modulation of the polarization state).

The developed theoretical model is quite general. It does not require the complete information about the nature and properties of photoactive anisotropic impurity centers responsible for PIE and about the features of charge transfer between them. Thus, it can be used for other garnets as well as for other ordered materials.

Acknowledgement

Financial support by the FWF, project P-15642 is acknowledged.

References

1. V.F.Kovalenko and E.L.Nagaev, Sov.Phys.Usp, 29, 297 (1986).
2. A.B.Chizhik, I.I.Davidenko, A.Maziewski and A.Stupakiewicz, Phys.Rev.B, 57, 22 (1998).
3. A.Stupakiewicz, A.Maziewski, I.Davidenko and V.Zablotskii, Phys.Rev.B, 64, 064405 (2001).
4. V.A.Bedarev and S.L.Gnatchenko, Low Temp.Phys., 20, 124 (1994).
5. I.I.Davidenko, M.Fally, R.Rupp and B.Sugg, OSA Trends in Optics and Photonics, 62, 528 (2001).
6. I.I.Davidenko, N.A.Davidenko and S.L.Gnatchenko, Phys.St.Sol.(a), 189, 631 (2002).
7. I.I.Davidenko, M.Fally and R.Rupp, Journal of Magnetism and Magnetic Materials, 226-230, 958 (2001).
8. J.F.B.Hawkes and R.W.Teale, J.Phys.C, 5, 481 (1972).
9. J.C.Slonczewski, Phys.Rev., 110, 1341 (1958).